Journal of Sol-Gel Science and Technology 33, 229–239, 2005

Anti-Microbial Hydroxyapatite Particles Synthesized by a Sol–Gel Route

REN-JEI CHUNG
Department of Materials Science and Engineering, National Tsing Hua University, 101, Sec 2, Kuang –Fu Road, Hsinchu 300, Taiwan, Republic of China

MING-FA HSIEH*
Biomedical Engineering Center, Industrial Technology Research Institute, 195 Sec 4, Chung Hsing Rd., Chutung, Hsinchu 310, Taiwan, Republic of China
mfhsieh@itri.org.tw

KUO-CHANG HUANG
Department of Materials Science and Engineering, National Tsing Hua University, 101, Sec 2, Kuang –Fu Road, Hsinchu 300, Taiwan, Republic of China

LI-HSIANG PERNG
Department of Chemical Engineering, Cheng Shiu University, 840, Chengcing Rd., Niaosong Township, Kaohsiung 833, Taiwan, Republic of China

FONG-IN CHOU
Nuclear Science and Technology Development Center, National Tsing Hua University, 101, Sec 2, Kuang –Fu Road, Hsinchu 300, Taiwan, Republic of China

TSUNG-SHUNE CHIN
Department of Materials Science and Engineering, National Tsing Hua University, 101, Sec 2, Kuang –Fu Road, Hsinchu 300, Taiwan, Republic of China

Received February 25, 2004; Accepted August 18, 2004

Abstract. Sol–gel route was applied to synthesize anti-microbial hydroxyapatite (HAp) powders by the addition of silver 200–20000 ppm or zinc salts. The bacteria strain, *Streptococcus mutans* (*S. mutans*, ATCC 25175) was used in the anti-bacterial tests. HAp phase was reproducibly obtained by the preparation conditions: $Ca(NO_3)_2$-$4H_2O$ and triethyl phosphate as sources of calcium and phosphorus sources, respectively, and ethanol as the solvent, aging for 16 h at 80°C, gelation and drying at 80°C for 24 h, then calcining at above 350°C. TGA was used to analyze thermal properties of the as-prepared gel. XRD and FTIR were used to identify the crystalline phase and chemical structure. CaO appeared as an impurity after calcining above 650°C. In the solid-state anti-microbial tests on the brain heart infusion (BHI) agar plates, there formed a microbial inhibition zone surrounding the Ag/Zn added (greater than 2000 ppm) samples. In the liquid-state anti-microbial tests, *S. mutans* cells readily precipitated with pure HAp powders but not with Ag/Zn added (greater than 2000 ppm) HAp powders. The concentration of silver or

*To whom all correspondence should be addressed.

zinc ions releasing from the Ag/Zn added HAp powders into the supernatant of the BHI broth was under detection limit of ICP-AES analyses. However, the growth of *S. mutans* reached same magnitude (6×10^8 CFU/mL) whether pure HAp, 2000 ppm-Ag or 2000 ppm-Zn were added. Therefore, Ag/Zn added HAp powders developed in this research present microbial inhibition properties and are of potential as a solid-state anti-microbial agent.

Keywords: hydroxyapatite, silver, zinc, sol–gel route, anti-microbial tests, *Streptococcus mutans*, short-range microbial inhibition

1. Introduction

Hydroxyapatite is the major inorganic component in natural bones [1, 2]. Because HAp has the advantages of excellent biocompatibility, free of cell toxicity, and forming strong bonding to bone osteoinductively, it has been widely studied and prepared in many forms for orthopedic and dental applications [3, 4]. There are many methods to synthesize HAp, including chemical precipitation [5], solid-state reaction [6], hydrothermal synthesis [7], sol–gel route, and so on [8, 9, 10].

For hard tissue replacement or fracture fixation, titanium-based alloy (such as Ti6Al4V) is the most common choice. In order to improve the bone-conduction ability and to enhance the primary healing stage, HAp coating has been widely applied onto the surface of metallic implants [10]. The thermal oxidation and thermal stress of metallic substrates are important factors of concern. Therefore, lower temperature processes such as sol–gel processing [12, 13] or electrodeposition [11] draw much attention recently. Not only biomedical applications, anti-microbial coatings also play extremely important roles in daily usages, such as coatings onto surface of basin or grip. In this study, a sol–gel route was applied to synthesize HAp with extra addition of silver and/or zinc ions. Synthetic routes and optimal processing parameters (conditions) were investigated.

Most implants are applied intact with human tissue directly, infections after orthopedic surgery are frequent and serious, so that biomaterials with anti-bacterial capability provide merits of less infectious chances hence extend the preservation period as well as it's applicability. There are a few studies in the delivery of antibiotics to the interface, and HAp was found to serve as an efficient carrier [14, 15]. Among the antibiotics, ionic heavy metals are efficient, comparatively stable with respective to organic ones, and being carried by HAp through ionic substitution. They are Ag^+, Zn^{2+} and Cu^{2+}, etc. [16–18]. Ag^+ is a widely and regularly used anti-bacterial element. Zn^{2+} is also reported to be an anti-bacterial element, being abundant in human body, with specialized and passive effects on osteo-metabolism [19, 20]. We chose Ag^+ and Zn^{2+} as the antibacterial candidates to partly substitute Ca^{2+} ion in HAp. For the adding of anti-microbial ion into hydroxyapatite, most of the published literature utilized an ionic exchange process. However, the anti-microbial agent would just accumulate onto the surface and led to rapid releasing and also with higher toxicity [14, 16, 21]. Through sol–gel route the substituted ions would directly insert into the HAp lattice [22, 23] and provide stable compound due to the extreme little dissolution property of HAp [14, 24]. A well and homogenously substituted HAp was expected as a good slow releasing carrier. In this study, an etiological agent of human caries and plaques [25], *Streptococcus mutans* (ATCC 25175), was used in the anti-bacterial *in vitro* tests.

2. Materials and Methods

2.1. HAp Powders Derived Through Sol–Gel Processes

HAp precursors were prepared by mixing $Ca(NO_3)_2$-$4H_2O$ (Merck Co., Germany) and triethyl phosphate (TEP, Janssen Chimica, Belgium) in anhydrous ethanol (99.9%, Riedel-deHaen Co., Germany). The atomic ratio of Ca to P was 1.67. The details of precursor preparation was published elsewhere [9]. $AgNO_3$ (Merck Co., Germany) and $Zn(NO_3)_2$-$6H_2O$ (Riedel-deHaen Co., Germany) were added in the precursors as antimicrobial agents, respectively. The amounts added in the precursors were 200 to 20000 ppm by atomic ratio versus calcium atoms. The precursors were aged at 80°C for 16 h, followed by gelation for 24 h and dried at 80°C. During the aging step, pH values of the solutions were recorded. The viscosity of the precursor at 25°C was measured by a cone-and-plate viscometer

(DVIII+, Brookfield, USA) having measurement range from a few cP (centipoises) to 10^5 cP. A sol is defined to be a clear fluid; while a gel non-transparent semi-solid.

The as-dried gels were then calcined at different temperatures (250 to 650°C) with a heating rate 5°C/min, kept for 30 min, and then air-cooled. Calcined powders were abbreviated as 200 ppm-Ag, 2000 ppm-Ag, 20000 ppm-Ag, 200 ppm-Zn, 2000 ppm-Zn, and 20000 ppm-Zn, respectively.

2.2. *Materials Characterizations*

Thermogravimetric analyses (TGA) of the gels were carried out using a thermal analyzer (SSC 5200, Seiko Co., Japan) from room temperature to 1200°C under an air flux of 100 mL per minute ramping at 5°C/min.

Crystalline phases of the calcined powders were investigated using X-ray powder diffraction method (maxIIB, Rigaku Co., Japan). X-ray radiation of Cu K_α (0.1548 nm) was set at 30 kV and 20 mA with a Ni filter. To determine the crystalline phases of the specimens, a 2θ scanning range from 20 to 60 degree was used with a scanning speed 4 degree per min. The crystalline phases was identified by comparing with JCPDS files (HAp: 09-0432, CaO: 37-1497, $CaCO_3$: 05-0586, AgO_2: 19-1155). The structural identification of calcined powders was also investigated by a Fourier transform infrared spectrometer (FTIR). 3 mg of calcined powders, mixed with 0.3 g KBr, were compacted by a hydraulic press. For each spectrum, 32 scans between 400–4000 cm^{-1} were procured.

Morphology of the powder was observed using a field emission scanning electron microscope (FE-SEM, model JSM-6500F, Jeol, Japan). The atomic Ca/P ratio of the calcined HAp was analyzed by inductively coupled plasma-atomic emission spectroscopy (ICP-AES, 4100DV, Optima, USA) after being digested by a microwave oven (mls 1200, Milestone Co., Italy).

Ions releasing behavior of the calcined powders in the bacterial culture medium were analyzed by ICP-AES. After immersing 0.05 g powders in the medium for 72 h, the supernatant was separated by a centrifuge at 5000 rpm, 10 min and concentrations of Ca, P, Zn and Ag were then analyzed.

2.3. *Establishment of Normal Cultivation of Streptococcus mutans (S. mutans)*

S. mutans (ATCC 25175), obtained from official cell bank in Taiwan (Bioresources collection and research center), was steadily cultured at 37°C in brain heart infusion broth (BHI, Difico. Co., USA). To determine normal growth curve of *S. mutans* for a period up to 80 h, aliquot amount of cell suspension was sampled, diluted and then spread on brain heart infusion agar plates (BHIA, Difico. Co., USA) for 48 h and then served to colony formation unit (CFU) counting. The time course of microbial growth was then calculated.

2.4. *Anti-Microbial Tests*

In order to prevent contamination from other biological species, powders applied in anti-microbial tests were sterilized with gamma irradiation at the dosage of 10 KGy (the Isotope Division, Nuclear Science and Technology Development Center, National Tsing Hua University, Taiwan). The anti-microbial effects were tested in both solid and liquid media. *S. mutans* was cultured to exponential growth stage after being thawed from freezer. The liquid state tests can indicate the interaction of calcined powders and bacteria and understand whether releasing of added Ag/Zn salts into the medium can be harmful to *S. mutans*. The solid-state tests aimed to investigate the anti-microbial zone, within it the proliferation of *S. mutans* was retarded, and it helped us to judge *S. mutans* would directly grow onto the calcined powders or not.

In the solid-state tests, 10^4 CFU *S. mutants* cells were spread on the BHIA plates; compacted powders (made of 0.05 g calcined powders, 5 mm in diameter, pressed by 10 kgf/cm^2, 30 sec) were then arranged to the agar surface and incubated for 48 h. The microbial inhibition zone was observed under optical microscope. For liquid state tests, 0.05 g powders (pure or Ag/Zn added) were suspended into 5 mL BHI broth containing 5×10^5 CFU/mL *S. mutans* cells. After a certain time interval, the total cell number was counted and also described as CFU/mL.

3. Results and Discussion

3.1. *Sol–Gel Process and Calcining Conditions*

A sol–gel process for preparing powders includes the following steps: (1) molecular mixing of the precursors to form a clear solution; (2) hydrolysis reaction initiates; (3) condensation of the hydrolyzed species and then forming meta-stable structures; (4) elimination of the solvent and resulting immobile non-transparent gel;

(5) removal of residual organic components through calcining and leave aim products.

The mixture of precursors was a homogenous solution and its viscosity was increasing from around 7 cP to an over-range value after drying for 1 to 6 h. For the precursor dried for 3–4 h, the viscosity fell in between 14–20 cP, depending on the value at room temperature during drying. The pH value of sol decreased obviously from 4.0($\pm$0.1) to 1.8($\pm$0.1) during aging. It is due to the hydrolyzation of TEP; H^+ evolved from TEP acidify the precursor solution. Liu et al. reported the reaction [26]:

$$\begin{aligned}&PO(OEt)_{3-x}(OH)_x + Ca^{2+} + NO_3^- \\ &\quad \rightarrow (NO_3)^-(OH)\text{-}Ca\text{-}O\text{-}PHO(OEt)_{3-x}, + H^+ \\ &\quad + C_2H_5OH + H_2O\end{aligned}$$

Further, regardless of Ag/Zn addition in the precursors, pH changes showed no difference. This may indicate that Ag/Zn ions play no role on Ca-phosphate gelling network.

In order to understand the thermal properties of prepared gel after drying for 24 h, thermogravimetric analyses were conducted. A typical TGA diagram is shown in Fig. 1. The apparent weight loss before 300°C is attributed to the exhaust of solvent and decomposition into volatile smaller molecules. The second step weight loss between 300 to 600°C is due to the decomposition of larger organic molecules and residual components. For all the studied samples, the TGA analyses didn't show manifest differences among each other no matter Ag-/Zn-added or not. It implies the small amount of additives do not substantially affect the phase forming ability and synthetic process.

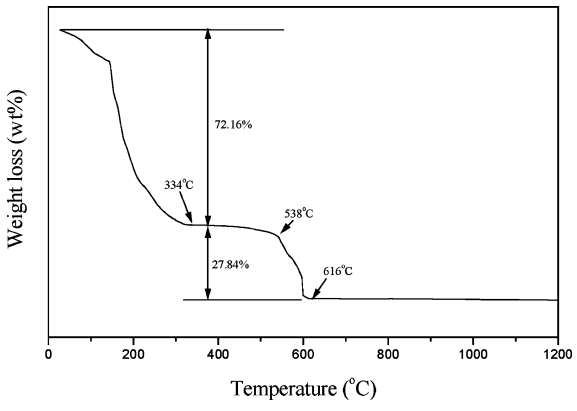

Figure 1. TGA curve of precursor with no Ag/Zn added. Most of the residents were burned out above 600°C.

3.2. *Crystalline Phases of Calcined Powders*

XRD patterns (Fig. 2(a)) show that phase of HAp formed when calcined above 350°C. Crystallinity of HAp improves with increasing calcining temperature. And CaO appears after calcining above 650°C. It is due to incompletely reacted precursors and intermediates, such as $Ca(NO_3)_2$, $CaCO_3$, and $Ca_3(PO_4)_2$ [9]. Figure 2(b) shows XRD patterns of calcined powders with Ag/Zn added after calcining at 600°C. Every sample has HAp crystalline phase, and there is no other crystalline phase besides 20000 ppm-Ag sample. Ag_2O and CaO peaks can be observed when Ag addition reached 20000 ppm.

The present study used silver nitrate as Ag source. Silver nitrate in sol–gel matrix can be calcined to various oxidation states. For instance, Traversa et al. calcined $AgNO_3$ containing TiO_2 gel at elevated temperatures (300–600°C) resulted in silver carbonate and silver nitrate. They also found reduced silver atoms from X-ray photoelectron spectroscopy [27]. The processing temperatures were not high enough for lattice incorporation. Instead, ionic attraction between its counterparts, such as carbonate, dominated formation of silver derivatives. Katakam et al. compared silver formation in HAp materials by microwave heated or conventional sintered Ag_2O-HAp materials at 900°C [28]. They found that Ag_2O was reduced to metallic silver. However, HAp was also transformed to biphasic HAp and tricalcium phosphate.

In our study, we adopted low-temperature sol–gel route. Lattice incorporation of metallic silver in HAp lattice might not happen. Thus Ag_2O formed in our system was due to electrostatic attraction with HAp.

The Ca/P ratio follows the ideal stoichiometry that is 1.67 by ICP/AES analysis, and Ag/Zn to Ca ratio is extremely close to the designed composition. Figure 3 is the SEM micrograph of pure HAp powder. It reveals that the powders have average sizes ranging from 3 to 10 μm.

3.3. *FTIR Absorption Studies*

Figure 4 summarizes FTIR spectra of pure and modified HAp, i.e. 200 ppm-Ag, 2000 ppm-Ag, 20000 ppm-Ag, 200 ppm-Zn, 2000 ppm-Zn, and 20000 ppm-Zn, respectively. The presented significant absorbance agreed with HAp component in all powders [21]. Major characteristic HAp bands are assigned as: ν_1 PO_4^{3-} band around 962 cm^{-1}; ν_2 PO_4^{3-} band around 472 cm^{-1}; ν_3

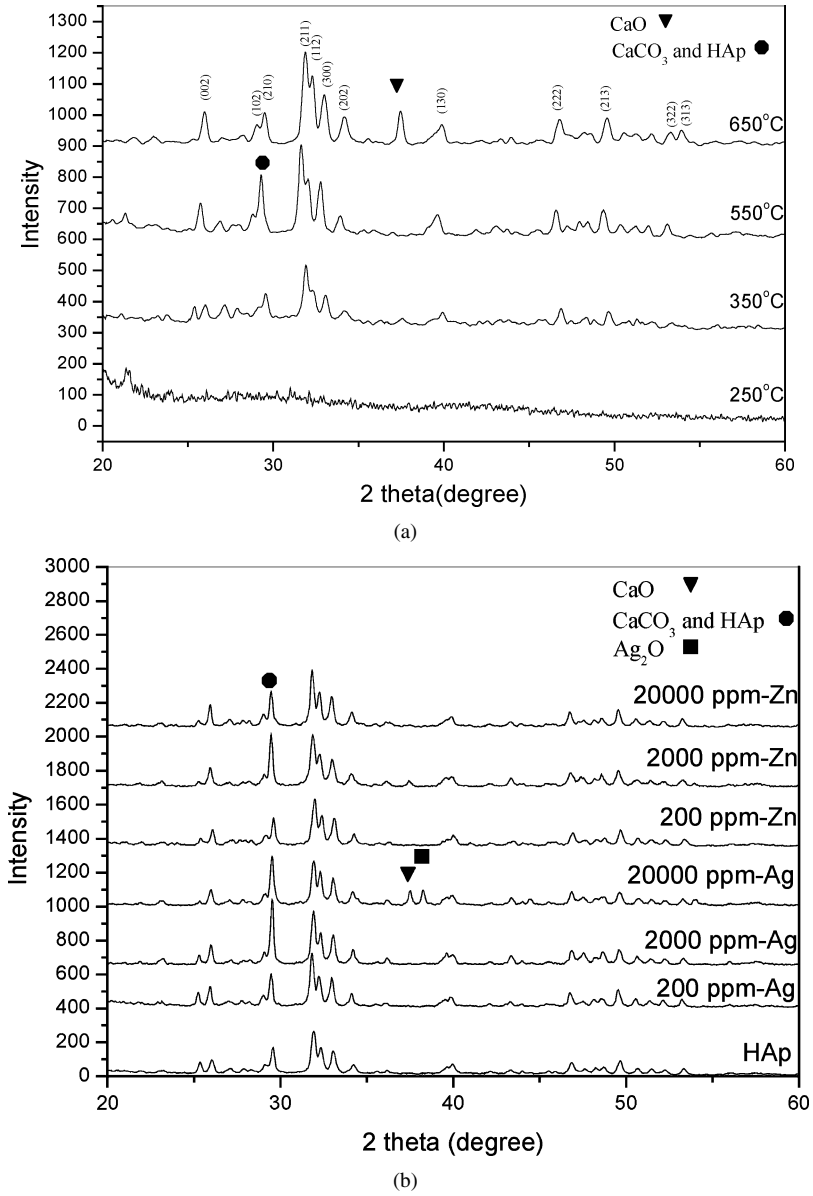

Figure 2. (a). XRD patterns of powders derived from precursors without Ag/Zn added calcined at different temperatures, HAp crystalline peaks were asssinged according to JCPD 24-0033. (▼ CaO, ● $CaCO_3$ (Calcite) and HAp, other peaks belong to HAp) Typical HAp peaks appeared when calcined above 350°C. CaO impurity would be produced above 650°C. (b). XRD patterns of powders after calcining at 600°C (▼CaO, ●$CaCO_3$ (Calcite) and HAp, ■ Ag_2O, other peaks belong to HAp) Besides 20000 ppm-Ag HAp was with Ag_2O and CaO impurity, every sample presented only typical HAp crystalline peaks.

PO_4^{3-} band around 1035 and 1096 cm^{-1}; ν_4 PO_4^{3-} band around 565, 574 and 603 cm^{-1}; adsorbed water and hydroxyl groups of broad absorption around 3500 cm^{-1}. Beside the typical HAp functional groups, there appeared other absorption bands. At 873 cm^{-1}, there is a ν_2 CO_3^{-2} vibration mode absorption. And carbonate group, such as ν_1 CO_3^{-2} , ν_1 CO_3^{-2} and C─O stretching, showed a broad absorption band around 1500 cm^{-1}. On the other hand, absorption band at 1380 cm^{-1} is assigned to be NO^{3-}. The carbonates and nitrate came from the residual of calcined precursors. For zinc-added powders, there is no Zn─O stretching located

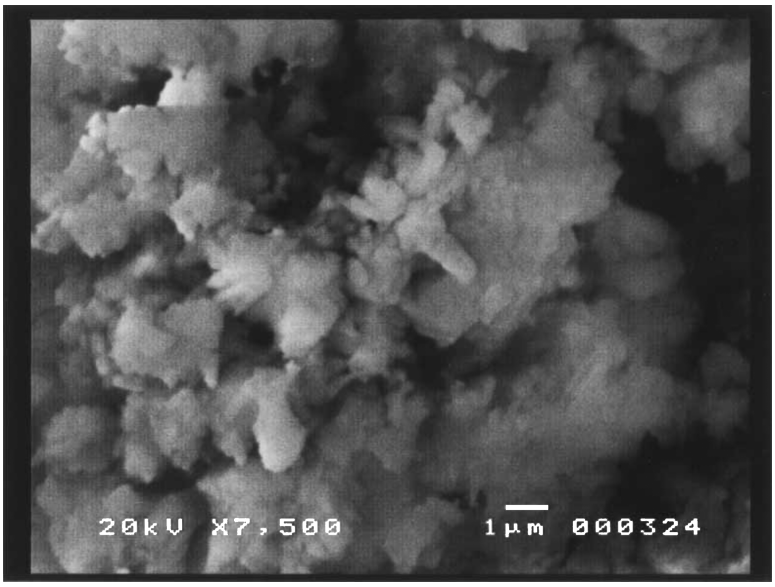

Figure 3. An SEM micrograph of calcined powder without addition showed that the particles sizes were ranging from 3 to 10 μm.

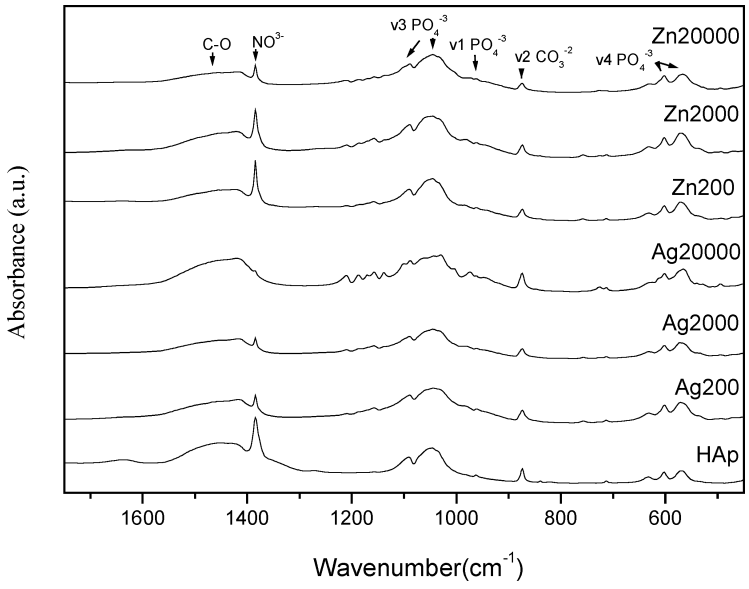

Figure 4. FTIR spectra of calcined HAp powders.

around 400 cm^{-1}. This is cross-verified to XRD patterns of Zn-added powders showing free of zinc oxide phase (Fig. 2(b)).

3.4. Establishment of Cell Culture of S. mutans

Cells of *S. mutans* being thawed from freezer were incubated at 37°C in BHI broth. Growth of the *S. mutans* culture at different time intervals was observed to determine the growth curve and doubling time. Moreover, morphologies of colony and cell pellet under liquid/solid cultures were also recorded, respectively. Figure 5 shows the growth curve of *S. mutans* in BHI. The doubling time was 2 h, and the maximum cell concentration reached 6×10^8 CFU/mL in BHI from initial of 5×10^5 CFU/mL after 24 h.

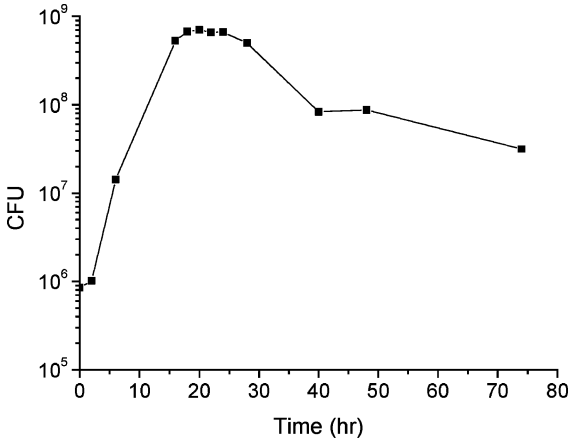

Figure 5. Growth curve of *S. mutans* in BHI without calcined powders.

The cell bodies precipitated at the bottom of the culture tube. When the cultivation reached stationary phase (6×10^8 CFU/mL) under regular static culture a condensed cell pellet was observed (Fig. 6). Cultivations of *S. mutans* on solid BHIA plate resulted in white colonies on BHIA. The radius of colonies was around 0.1–3 mm, and a higher plating density would lead to smaller colonies.

3.5. Solid-State and Liquid-State Antimicrobial Tests of Calcined Powders

As for the solid-state anti-microbial tests of the calcined powders, *S. mutans* grew directly onto pure HAp compact disk (Fig. 7) on BHIA plates. There was not any obvious barrier between the pure HAp disk and bacterial colonies. However, for 2000 ppm-Ag, 20000 ppm-Ag, 2000 ppm-Zn and 20000 ppm-Zn samples, *S. mutans* didn't grow into a circular region near the samples on BHIA (Figs. 8 and 9), thus microbial inhibition zones were manifest. Based on this observation, samples with Ag or Zn added more than 2000 ppm are ended up in toxicity to *S. mutans*. This contact inhibition is known to the most anti-bacterial phosphate salts [16]. Because silver ions can react with sulfur atom on nucleic acids or proteins of bacteria. Once contacted with materials, cells may uptake silver ions into cell body, resulting in perturbed physiological functions of cells. Higher additives or over-exposure of antimicrobial materials finally lead to cyto-toxicity to *S. mtans*.

For testing the Ag and Zn releasing from Ag/Zn added HAp in BHI broth, pure HAp, 2000 ppm-Ag and 2000 ppm-Zn calcined powders (0.05 g) were immersed in 5 mL BHI broth without *S. mutans* for 72 h. The materials finally precipitated at the bottom

Figure 6. Without calcined powders, *S. mutans* cell bodies precipitated beneath the cultural tube as circled.

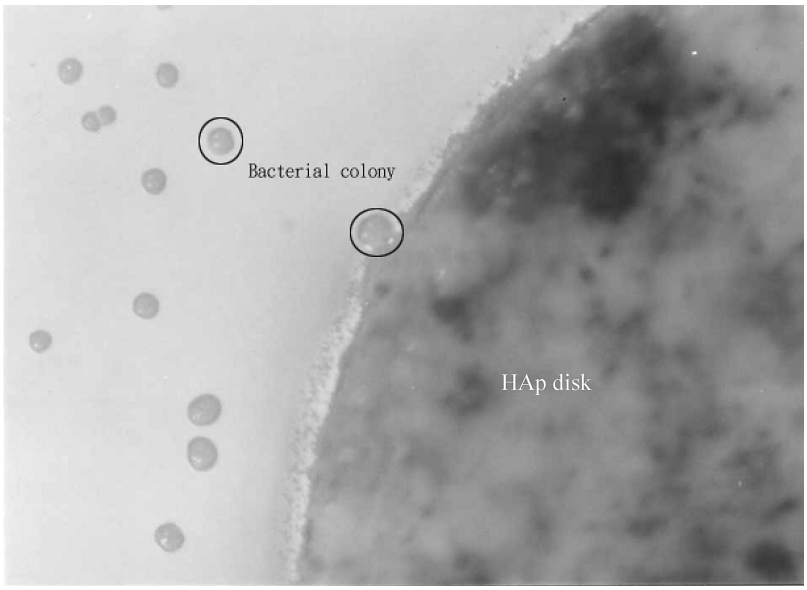

Figure 7. *S. mutans* grew onto pure HAp on BHIA plate, and examples of bacterial colony were circled.

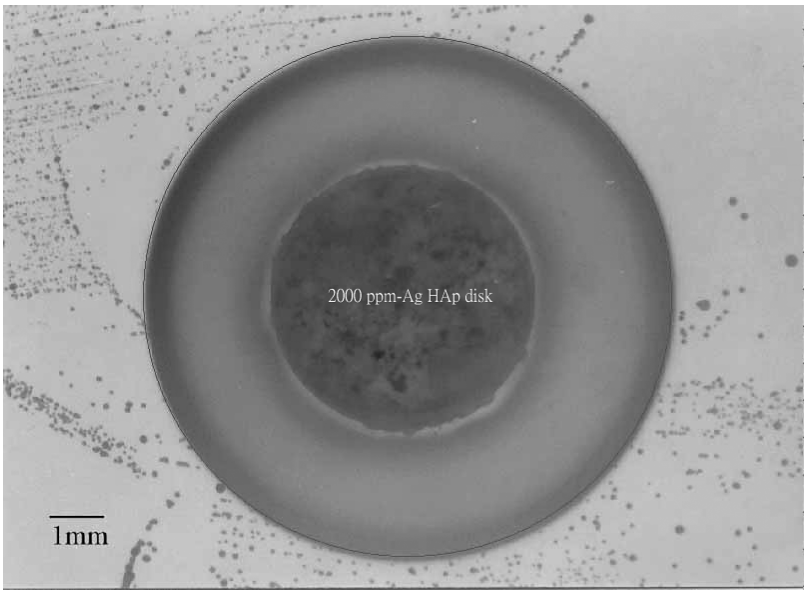

Figure 8. Microbial inhibition zone (circled) formed around the 2000 ppm-Ag HAp disk on BHIA plate with *S. mutans* cultured.

of the test tubes due to high density of calcium phosphates (>3 g/mL). The medium remained clear, and the supernatant was sampled for Ag or Zn analysis. Results showed that the concentration of Ag and Zn was under detection limit of ICP-AES. This meant that there was not any detectable Ag/Zn released into BHI broth within three days.

In liquid-state antimicrobial tests, the three kinds of aforementioned calcined powders (pure HAp, 2000 ppm-Ag and 2000 ppm-Zn) were suspended in 5 mL BHI broth together with *S. mutans* (seeding concentration 5×10^5 CFU/mL). After 24 h cultured, total cell number of the *S. mutans* in each culture reached 6×10^8 CFU/mL as the untreated ones in stationary phase after

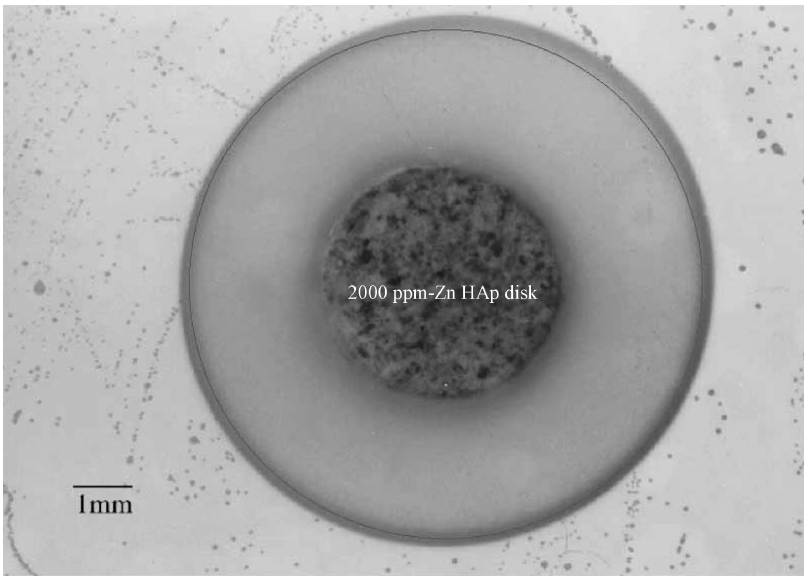

Figure 9. Microbial inhibition zone (circled) formed around the 2000 ppm-Zn HAp disk on BHIA plate with *S. mutans* cultured.

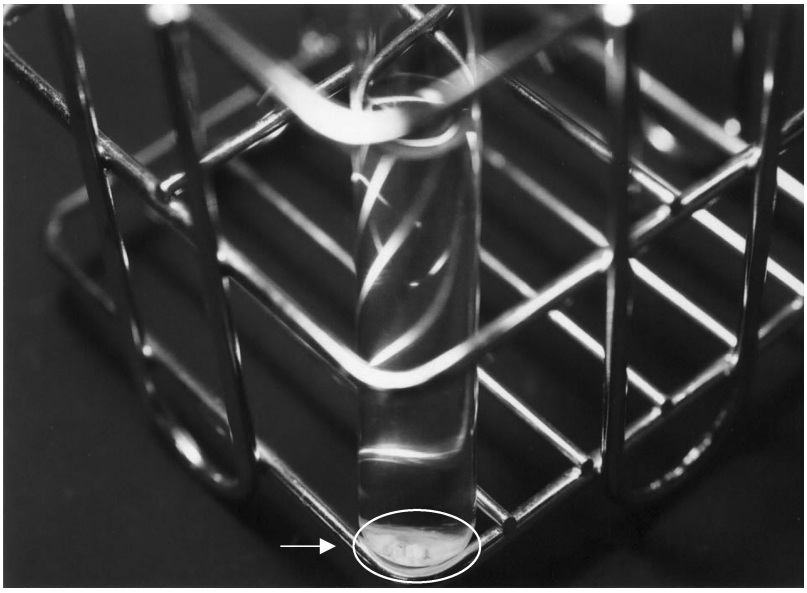

Figure 10. *S. mutans* precipitated with pure HAp powders in BHI indicated by the arrow. Above the precipitate, the medium remained clear.

practical surface plate counting. It meant that bacteria remained proliferating in BHI broth during culture period either when pure HAp or Ag/Zn added HAp existed.

Furthermore, an interesting phenomenon was observed. *S. mutans* would precipitate with pure HAp powders as indicated by an arrow (Fig. 10). Above the precipitate the medium showed a clear solution. However, when 2000 ppm-Ag and 2000 ppm-Zn powders were put into the said cultural test tube for 24 h, the microbial suspended homogenously, and turbid cultivations appeared (Figs. 11 and 12).

According to the cell counting, the total cell number in the culture of the *S. mutans* reached same magnitude (6×10^8 CFU/mL) whether pure HAp, 2000 ppm-Ag or 2000 ppm-Zn were added. Turbid medium

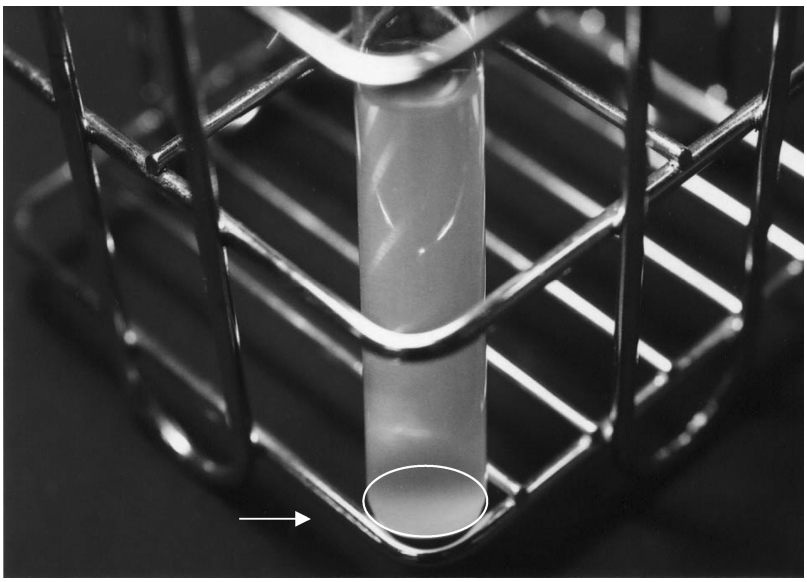

Figure 11. *S. mutans* would not precipitate with the 2000 ppm-Ag HAp powders (circled and indicated by the arrow) in BHI, and above the precipitate a homogenous turbid solution with a OD value as the saturated cultivation was presented.

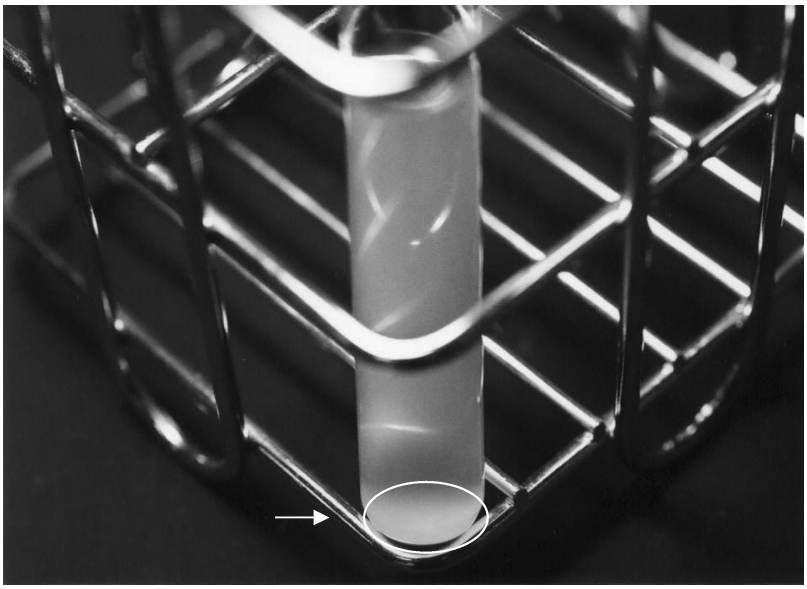

Figure 12. *S. mutans* would not precipitate with the 2000 ppm-Zn HAp powders (circled and indicated by the arrow) in BHI, and above the precipitate a homogenous turbid solution with a OD value as the saturated cultivation was presented.

revealed less *S. mutans* precipitated with Ag/Zn added HAp comparing to pure HAp. These phenomena implied that Ag/Zn added HAp powders would affect the characteristics of *S. mutans* in BHI culture and lead the cells to remain suspending. The detail mechanism is interesting and remaining further study.

4. Conclusions

Sol–gel route is a useful technique to synthesize Ag-/Zn-modified hydroxyapatie (HAp) particles. With ethanol as the solvent, HAp can be derived after the gels being calcined at 350°C. Further calcining above

650°C will lead to appearance of CaO because of the incompletely reacted precursors and intermediates. For the calcined powders, addition of minor amount of silver or zinc will not cause manifest mechanism changes during the calcining processes. The samples added with more than 2000 ppm-Ag or 2000 ppm-Zn will cause obvious microbial inhibition zone on BHIA plates with *S. mutans*, while however *S. mutans* will grow onto pure HAp disk. In BHI broth, *S. mutans* will precipitate with pure HAp, but remain suspending when 2000 ppm-Ag or 2000 ppm-Zn calcined powders exist after 24 h cultivation. Analyses of cell densities and released ions show that the added samples will not release detectable Agor Zn. *S. mutans* in liquid state culture reached same magnitude (6×10^8 CFU/mL) whether pure HAp, 2000 ppm-Ag or 2000 ppm-Zn were added, but the character of *S. mutans* seemed to be changed. The developed processes and HAp powders in this study reveal contact microbial inhibition, and are suitable for application on coatings and other antibacterial applications.

Acknowledgments

The authors are grateful for the sponsor of this research by the National Science Council of the Republic of China, under the grant NSC 91-2216-E-230-001 and NSC92-2216-E-230-003, and in part NSC91-2216-E -239-001.

References

1. P. Frayssinet, J.L. Trouillet, N. Rouquet, E. Azimus, and A. Autefage, Biomaterials **14**, 423 (1993).
2. M. Jarcho, C.H. Bolen, M.B. Thomas, J. Bobick, J.F. Kay, and R.H. Doremus, J. Mater. Sci. **11**, 2027 (1976).
3. H. Aoki, *Medical Application of Hydroxyapatite* (Takayama Press, St. Louis, 1994).
4. M. Jacho, Clin. Orthop. Rel. Res. **157**, 259 (1981).
5. T.A. Cuney, F. Korkusuz, M. Timicin, and N. Akkas, J. Mater. Sci. Mater. Med. **8**, 91 (1997).
6. R.R. Ramachandra, H.N. Roopa, and T.S. Kannan, J. Mater. Sci. Mater. Med. **8**, 511 (1997).
7. H.S. Liu, T.S. Chin, L.S. Lai, S.Y. Chiu, K.H. Chung, C.S. Chang, and M.T. Lui, Ceram. Int. **23**, 19 (1997).
8. C.S. Chai, K.A. Gross, and B. Ben-Nissan, Biomaterials **19**, 2291 (1998).
9. M.F. Hsieh, L.H. Perng, T.S. Chin, and H.G. Perng, Biomaterials **22**, 2601 (2001).
10. M.F. Hsieh, L.H. Perng, and T.S. Chin, J. Sol–Gel Sci. Tech. **23**, 205 (2002).
11. C.M. Cotell, Appl. Surf. Sci. **69**, 140 (1993).
12. W.J. Weng, G. Shen, and G.R. Han, J. Mater. Sci. Lett. **19**, 2187 (2000).
13. M.F. Hsieh, L.H. Perng, and T.S. Chin, Mater. Chem. Phys. **74**, 245 (2002).
14. M. Shirkhanzadeh, M. Azadegan, and G.Q. Liu, Mater. Lett. **24**, 7 (1995).
15. Q.L. Feng, T.N. Kim, J. Wu, E.S. Park, J.O. Kim, D.Y. Lim, and F.Z. Cui, Thin Solid Films **335**, 214 (1998).
16. T.N. Kim, Q.L. Feng, J.O. Kim, J. Wu, H. Wang, G.C. Chen, and F.Z. Cui, J. Mater. Sci. Mater. M. **9**, 129 (1998).
17. H. Aoki, *Science and Medical Application of Hydroxyapatite* (JAAS, Tokayama Press System Centre Co., Inc., 1991), p. 11.
18. S.H. Choi, K.S. Min, and J.W. Choi, *Hydroxyapatite Super Fine Powder Fabrication* (91st Advanced Engineering, Research Report (New Materials), Han Yang University, Korea, 1992), p. 10.
19. H. Kawamura, A. Ito, S. Miyakawa, P. Layrolle, K. Ojima, H. Naito, N. Ichnose, and T. Tateishi, J. Biomed. Mater. Res. **50**, 184 (1993).
20. W.J. Bettger and B.L. O'dell, J. Nutr. **4**, 194 (1993).
21. R.N. Panda, M.F. Hsieh, R.J. Chung, and T.S. Chin, J. Phys. Chem. Solids **64**, 193 (2003).
22. K.S. Oh, K.J. Kim, Y.K. Jeong, and Y.H. Choa, Key Eng. Mat. **240**, 583 (2003).
23. T. Kanazawa, *Inorganic Phosphate Materials* (Elsevier Science Publishers, Amsterdam, the Netherlands, 1989).
24. I. Manjubala, M. Sivakumar, T.S.S. Kumar, and K.P. Rao, J. Mater. Sci. Mater. M. **11**, 705 (2000).
25. T. Lehner, *Immunology of Oral Disease* (Blackwell Sci. Publication, 1992), Chap. 2, 3, 4, and 6.
26. D.M. Liu, T. Troczynski, and W.J. Tseng, Biomaterials **22**, 1721 (2001).
27. E. Traversa, M.L. Di Vona, P. Nunziante, S. Licoccia, J.W. Yoon, T. Sasaki, and N. Koshizaki, J. Sol–Gel Sci. Tech. **22**, 115 (2001).
28. S. Katakam, D. Krishna, and T.S. Kumar, Mater. Lett. **57**, 2716 (2003).